Journal of Inorganic Biochemistry 200 (2019) 110805

Contents lists available at ScienceDirect

Journal of Inorganic Biochemistry

journal homepage: www.elsevier.com/locate/jinorgbio

Multifunctional coordination polymers based on copper with modified nucleobases, easily modulated in size and conductivity

Verónica G. Vegas[a], Noelia Maldonado[a], Oscar Castillo[b], Carlos J. Gómez-García[c], Pilar Amo-Ochoa[a,d,*]

[a] Departamento de Química Inorgánica, Universidad Autónoma de Madrid, 28049 Madrid, Spain
[b] Departamento de Química Inorgánica, Universidad del País Vasco (UPV/EHU), Apartado 644, E-48080 Bilbao, Spain
[c] Instituto de Ciencia Molecular (ICMol), Parque Científico, Universidad de Valencia, Catedrático José Beltrán, 2, 46980 Paterna, Valencia, Spain
[d] Institute for Advanced Research in Chemical Sciences (IAdChem), Universidad Autónoma de Madrid, Madrid 28049, Spain

ARTICLE INFO

Keywords:
Coordination polymer
Copper
Nucleobases
Magnetic and electrical properties
Nanoprocessing

ABSTRACT

In this work, three mono- and bidimensional coordination polymers (CPs) based on Cu(II) and Cu(I) ($[Cu_2(TAcO)_2(C_2O_4)(4,4'\text{-bpy})]\cdot 4H_2O$ (**CP1**), $[Cu_2(UAcO)_2(C_2O_4)(4,4'\text{-bpy})]\cdot 2H_2O$ (**CP2**) and $[Cu_2(TAcO)_2(4,4'\text{-bpy})]$ (**CP3**)), decorated with thymine and uracil-1-acetate (TAcO and UAcO), 4,4′-bipyridine (4,4′-bpy) and oxalate are synthetized. The supramolecular structures of the CPs are based on the formation of non-canonical hydrogen bonds established between the free moieties of nucleobases. Interestingly, the presence of Cu(II) centers provide for compound **CP1**, magnetism and semiconducting properties. Additionally, **CP1** has been doped with iodine, increasing its electrical conductivity up to two orders of magnitude. Moreover, the size of the materials can be modulated from millimeters to the nanoscale, depending on the crystallization conditions and/or using ultrasound.

1. Introduction

Coordination polymers (CPs) are a large family of compounds, generally formed by a metal cation and an organic ligand [1]. The possibilities of combining the building blocks are extraordinary and for about 50 years, researchers have been able to obtain more than 60,000 CPs with different structures and properties [2–5]. Despite these great advances in synthesis and characterization, new and interesting challenges have appeared for them, so within the wide variety of potential applications that these materials can present, very recently it has been described their ability as nanocarriers at the cellular level [6]. Indeed, if we want to use these materials in biological applications, the incorporation of organic ligands with molecular recognition capabilities in the CP structure is highly interesting [7]. Thus, the use of modified nucleobases can allow the generation of CPs with selective molecular recognition e.g. other nucleobases, other biological active sites [5] or molecules of pharmacological interest [8]. In addition, nanoprocessability of these CP materials (nano coordination polymers (NCPs)) is required, in order to incorporate them at the biological level. In this regard, there is already a considerable number of studies that take advantage of the great insolubility of the CPs to form them at the nanoscale, based on bottom-up strategies, using either rapid precipitation in poor solvents [9] or in the presence of surfactants among other alternatives [10,11]. There are also works that describe how to prepare these materials at the nanosize scale using top-down approaches. For instance, liquid phase exfoliation assisted by ultrasound [12,13] to reduce their size to the nanometer scale. In fact, in recent years interesting works have been published on functionalized nanoparticles with ligands of biological interest as nucleotides, peptides or proteins for medical or pharmacological purposes, however, although the manufacture of NCPs is a simpler and direct process, the use of NCPs for similar purposes has not been widely studied to date.

In order to obtain new functional CPs based on nucleobases it is highly important the selection of suitable building blocks and the synthetic procedures. In fact the use of unconventional synthetic methods such as solvothermal conditions, together with the presence of pyrimidine derivatives ligands and the variation of pH medium, have allowed in some cases the in situ transformation of the organic ligands [14] and favors changes in the metal ion oxidation states. This strategy can be very useful in the synthesis of new CPs with new and interesting properties [14,15]. Moreover, it has been recently demonstrated that the use of copper(II), generates low toxicity CPs with interesting magnetic [16,17] and electrical properties [18–22]. Additionally, to improve the properties of a given CP, the use of doping agents for the

* Corresponding author at: Departamento de Química Inorgánica, Universidad Autónoma de Madrid, 28049 Madrid, Spain.
E-mail address: pilar.amo@uam.es (P. Amo-Ochoa).

https://doi.org/10.1016/j.jinorgbio.2019.110805
Received 18 June 2019; Received in revised form 19 August 2019; Accepted 19 August 2019
Available online 20 August 2019
0162-0134/ Published by Elsevier Inc.

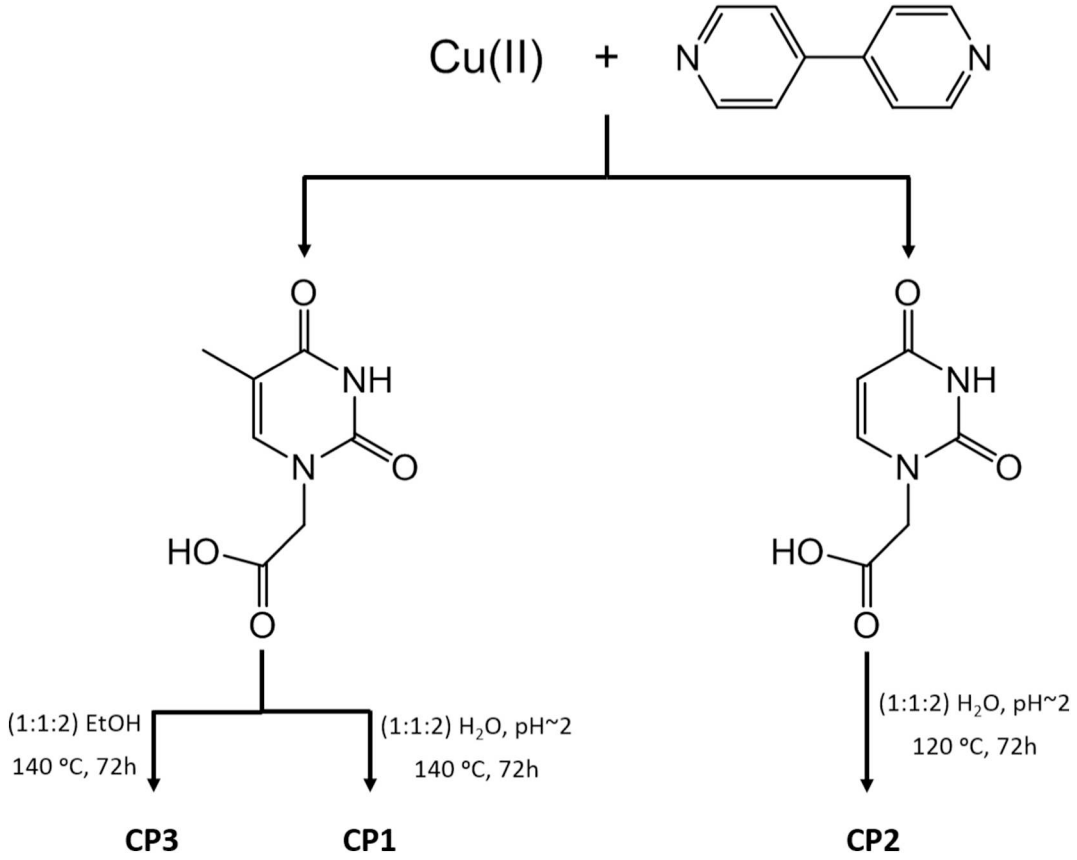

Fig. 1. Scheme of the synthetic conditions to obtain the CP **1–3**.

modulation of the electrical properties has been shown as a suitable tool [23].

In this study, we have selected modified uracil and thymine nucleobases with acetic acid located at N(1) position and copper as metal center for the formation of novel CPs. The modification with the carboxylic groups allows the coordination of the metal center while the nucleobase moiety is free available to form hydrogen bonds with other molecules (Fig. 1). The magnetic and electrical behavior of these CPs have been studied, as well as the modification of their electrical properties by doping. It has also been demonstrated the possibility of nanoprocessing them by top-down approach.

2. Materials and methods

All reagents and solvents were purchased from standard chemical suppliers: thymine-1-acetic acid (TAcOH) 98% and 4,4′-bipyridine (4,4′-bpy) 98% (Sigma-Aldrich). $Cu(NO_3)_2{\cdot}3H_2O$, $CuSO_4{\cdot}5H_2O$ and were used as received. Uracil-1-acetic acid (UAcOH) was synthesized as described in the literature [24].

Infrared spectroscopy (FT-IR) spectra were recorded on a PerkinElmer 100 spectrophotometer using a PIKE Technologies MIRacle Single Reflection Horizontal Attenuated Total Reflectance (ATR) Accessory from 4000 to 600 cm^{-1}.

Elemental analysis was performed on an elementary microanalyzer LECO CHNS-932. It works with controlled doses of O_2 and a combustion temperature of 1000 °C.

The X-ray diffraction data collection was done on a Bruker Kappa Apex II diffractometer with graphite-monochromated Mo Kα radiation (λ = 0.71073 Å). The cell parameters were determined and refined by a least-squares fit of all reflections. A semi-empirical absorption correction (SADABS) was applied. All the structures were solved by direct methods using the SIR92 program [25] and refined by full-matrix least-squares on F^2 including all reflections (SHELXL) [26] All calculations were performed using the WinGX crystallographic software package [27]. Crystal parameters and details of the final refinements of compounds **CP1**, **CP2** and **CP3** are summarized in Table S1.

Powder X-ray diffraction was collected using a PANalytical X'Pert PRO MPD θ/2θ secondary monochromator and detector with fast X'Celerator, which was used to general assays. Theoretical X-ray powder diffraction patterns were calculated using Mercury Cambridge Structural Database (CSD) version 4.0.0 software from the Crystallographic Cambridge Database. The samples were analyzed with scanning θ/2θ.

Thermal Gravimetric Analysis (TGA) was performed on a TGA Q500 Thermobalance with an evolved gas analysis furnace and mass spectrometer Thermostat Pfeiffer from Tecnovac, to analyze gases that are given off from the sample. The powder sample was analyzed using a Pt sample holder and N_2 flow as purge gas of 90 mL min^{-1} with a heating ramp from room temperature to 650 °C at 5 °C/ min.

Scanning Electron Microscopy (SEM) images were obtained with a Philips XL30 S-FEG scanning electron microscope. Aliquots of 40 μL of a **CP1** suspension were deposited on a SiO_2 surface to measure them.

Magnetic measurements were done in a Quantum Design MPMS-XL-5 superconducting quantum interference device (SQUID) magnetometer in the 2–300 K temperature range with an applied magnetic field of 0.5 T on polycrystalline samples of compound **CP1** with mass of 9.440 mg, respectively. The isothermal magnetization measurements were done with fields from −5 to 5 T at 2 K. Susceptibility data were corrected for the sample holder and for the diamagnetic contribution of the salts using Pascal's constants. Bain [28].

Direct current electrical conductivity measurements were performed on different single crystals, with graphite paste at 300 K and two contacts. The contacts were made with wolframium wires (25 μm diameter). The samples were measured at 300 K applying an electrical

current with voltages from +10 to −10 V. The electrical conductivity of iodine doped **CP1** was measured using the same technique and the same voltage range. Iodine doping was carried out by exposing **CP1** with iodine vapor at ambient temperature and pressure at different times, from 0 to 24 h.

2.1. Synthesis of $[Cu_2(TAcO)_2(C_2O_4)(4,4'\text{-bpy})]\cdot 4H_2O$ (CP1)

A mixture of $Cu(NO_3)_2\cdot 3H_2O$ (0.1 g, 0.41 mmol), thymine-1-acetic acid (TAcOH) (0.152 g, 0.82 mmol), and 4,4′-bpy (0.065 g, 0.41 mmol) was prepared in a total volume of 18 mL of water MilliQ, ($pH_i = 1.92$). The mixture is subjected to solvothermal conditions, in a sealed glass reactor, that consist of a heating ramp from room temperature to 140 °C at 1.2C min^{-1}, followed by an isotherm of 72 h and a cooling ramp to room temperature for 24 h. The co-crystallization of dark blue crystals of $[Cu(TAcO)_2(H_2O)(4,4'\text{-bpy})]n\ 2H_2O$ [6] and turquoise crystals (**CP1**), both with needle-shaped, are observed in the bottom of the reactor. The supernatant is removed ($pH_f = 3.06$) under vacuum and the turquoise crystals are separated manually from the dark blue (60% yield). Anal. Calcd. (found) for $C_{26}H_{26}Cu_2N_6O_{14}$: % C, 40.37 (40.64); % H, 3.39 (3.58); % N, 10.82 (10.86). The IR has the following characteristic bands (cm^{-1}): 3155 (w), 3021 (w), 2840 (w), 1659 (s), 1584 (s), 1470 (m), 1322 (m), 1225 (s), 1146 (w), 1078 (s), 962 (w), 827 (m), 767 (m), 712 (m), 645 (m). Powder X-ray diffraction confirms that the structure of the microcrystalline solid obtained in the reaction is the same as the obtained by single crystal X-ray diffraction (Fig. S1).

2.2. Nanoprocessing of CP1 via top-down approach

1.5 mg of **CP1** crystals (ca. 2 mm) were immersed in 3 mL of acetone and were sonicated with ultrasonic bath Elmasonic P 300H at 37 kHz and 100 W for 1 h. After that time, the sample was centrifuged at 3000 rpm for 2 min. Then, two aliquots of 40 μL of both, the suspension before centrifuging and the supernatant after centrifuging, were deposited on a SiO_2 surface to measure them. The characterization of the nanoprocessed sample has been carried out by IR spectroscopy and powder X-ray diffraction (Figs. S11 and S12).

2.3. Synthesis of $[Cu_2(UAcO)_2(C_2O_4)(4,4'\text{-bpy})]\cdot 2H_2O$ (CP2)

A mixture of $Cu(NO_3)_2\cdot 3H_2O$ (100 mg, 0.41 mmol), Uracil-1-acetic acid (UAcOH) (141 mg, 0.82 mmol) and 4,4′-bpy (65 mg, 0.41 mmol) was stirred in 18 mL of water (pH = 2.30) for 10 min at 25 °C. The resulting purple solution was heated at 120 °C for 3 days in a solvothermal reactor and cooled to 30 °C for ca. 38 h (at ca. 0.04 °C/min). The obtained light blue crystals that were unstable out of the mother liquor were dried under vacumm. Anal. Calcd. (found) for $C_{24}H_{20}Cu_2N_6O_{13}$: %C, 39.62 (39.46); % H, 2.75 (2.62); %N, 11.55 (11.32). The IR has the following characteristic bands (cm^{-1}): 3526 (w), 3174 (w), 3108 (w), 3054 (w), 3027 (w), 1658 (s), 1613 (s), 1585 (m), 1469 (m), 1421 (m), 1400 (m), 1380 (m), 1347 (m), 1322 (m), 1243 (m), 1205 (m), 1108 (w), 1078 (m), 958 (m), 824 (s), 762 (s), 725 (s), 650 (m), 596 (w). Powder X-ray diffraction confirms that the structure of the microcrystalline solid obtained in the reaction is the same as that obtained by single crystal X-ray diffraction (Fig. S4).

2.4. Synthesis of $[Cu_2(TAcO)_2(4,4'\text{-bpy})]$ (CP3)

A mixture of thymine-1-acetic acid (TAcOH) (76 mg, 0.41 mmol), 4,4′-bpy (64 mg, 0.41 mmol) and an aqueous solution (1 mL) of $Cu(NO_3)_2\cdot H_2O$ (100 mg, 0.41 mmol) was stirred in 12 mL of ethanol for 10 min at 25 °C. The resulting deep blue solution was heated at 140 °C for 72 h in a solvothermal glass reactor and cooled to 20 °C for ca. 2 h (at ca. 0.083 °C/min). The yellow crystals were filtered off and dried in vacuum (41% yield). Anal. Calcd. (found) for $C_{24}H_{22}Cu_2N_6O_8$: % C, 44.37 (44.45); % H, 3.39 (3.38); % N, 12.94 (13.03). The IR has the following characteristic bands (cm^{-1}): 3471 (w), 1685 (s), 1643 (s), 1608 (s), 1473 (m), 1427 (m), 1373 (m), 1351 (m), 1282 (m), 1247 (w), 1228 (s), 1151 (w), 1074 (w), 982 (w), 882 (m), 831 (s), 798 (m), 763 (s), 727 (w). Powder X-ray diffraction confirms that the structure of the microcrystalline solid obtained in the reaction is the same as that obtained by single crystal X-ray diffraction (Fig. S6).

3. Results and discussion

In this study we have used two different nucleobases, uracil-1-acetic acid (UAcOH) and thymine-1-acetic acid (TAcOH), all of them have been reacted with copper(II) as metal center in nitrate forms (Fig. 1).

The reactions are carried out in water or ethanol (EtOH), under solvothermal conditions. The control of the pH and stoichiometry are key factors determining the formation of the final compound [29]. The number of solvation water molecules present in **CP1** and **CP2** can be modulated depending on the drying conditions of the crystals obtained.

All the reactions were carried out under solvothermal conditions, in a 1:1:2 stoichiometric ratio, (copper(II), 4,4′-bipyridine and nucleobase) (see Fig. 1). The synthesis of **CP1** and **CP2** was carried out in water at pH around 2 and the presence of oxalate ($(C_2O_4)^{2-}$) in these compounds, acting as a bridging ligand, has been observed. These experimental observation, can be rationalized taken into account previous reports in which the use of solvothermal conditions, in combination with acid pHs and the presence of copper(II) as catalyst and reducing agent, produce an in situ decarboxylation of carboxyl groups. Thus, the carboxylic acid groups becomes CO_2, which promote to $(C_2O_4)^{2-}$ in the presence of Cu^{2+}, by a reduction reaction [30,31].

In case of **CP3** a reduction of Cu(II) to Cu(I) it has been also reported as a consequence of the use of ethanol as solvent (reducing agent) in the presence of pyrimidine derivatives under solvothermal conditions [15,32].

Clearly the oxygens of the carboxyl group have large affinity for the metal centers, being able to bond using different coordination modes, i.e. monodentate, chelate or bridge, among others (Fig. 2). Single crystal X-ray diffraction studies confirm the same bidentate bridge coordination mode in the case of the uracil and thymine-1-acetate (**CP1** and **CP2**), and bridge monodentate mode in the case of thymine-1-acetate, for **CP3**.

3.1. Structural studies by single crystal X-ray diffraction of CPs 1–3

Compounds **CP**1 and **CP2** consist of a corrugated 2D coordination polymer in which there is only one crystallographically independent copper(II) metal center and three different bridging ligands: μ-4,4′-bpy-κ*N*:κ*N*′, μ-RCOO-κ*O*:κ*O*′ and μ-oxalato-κ*O*,κ*O*′:κ*O*″,κ*O*‴ (Fig. 3). The 2D coordination polymer can be described as being composed of ladder-like columns in which the copper(II) metal centers are bridged by μ-oxalato-κ*O*,κ*O*′:κ*O*″,κ*O*‴ (5.2098(9) Å) and *syn-anti* coordinated μ-RCOO-κ*O*:κ*O*′ carboxylate (4.7559(3) Å) ligands to define the side rail and the rung of the ladder like column, respectively. These columns are further connected by μ-4,4′-bpy-κ*N*:κ*N*′ ligands to provide a corrugated 2D sheet. The coordination geometry around the metal center is conditioned by the Jahn-Teller effect of copper(II). It presents an elongated square pyramidal geometry. The basal plane, with bond distances around 1.94–2.00 Å, is occupied by two oxygen atoms from the bridging oxalato ligand, one nitrogen from the *bpy* ligand, and one carboxylate oxygen atom from the thymine/uracil-1-acetate ligand. The apical position, with a longer bond distance (2.18–2.20 Å) is occupied by the second carboxylate oxygen atom from a second functionalized nucleobase. There is also a Cu···O semicoordination bond (2.74–2.77 Å) involving one of the previously coordinated oxygen atoms from the carboxylate group. This combination of bridging ligand gives rise to a corrugated 2D coordination polymer with the thymine/uracil residues tethering the external surface of the sheet. As a result, these nucleobases are able to establish complementary hydrogen bonding

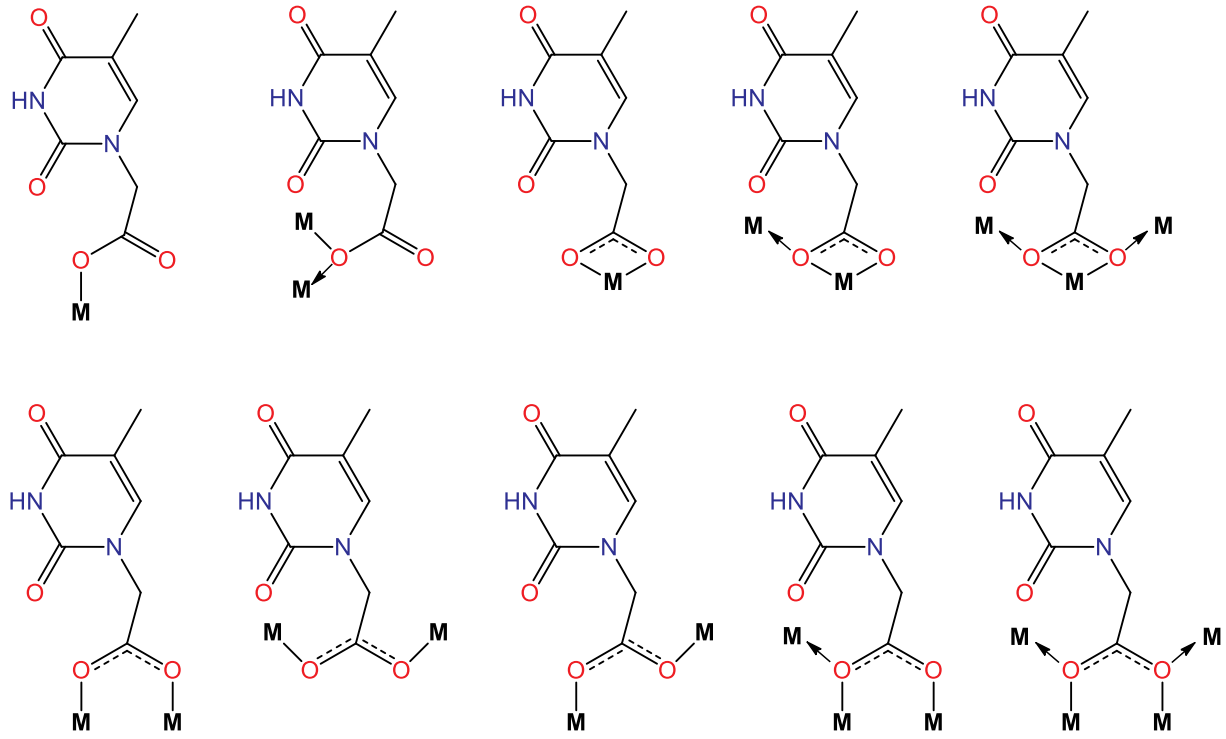

Fig. 2. General coordination modes of the carboxyl group oxygen to a transition metal center.

interactions among them (2 × N3-H···O2) to held the 2D sheets and provide the final 3D crystal architecture. The cohesiveness of the crystal building is reinforced by the presence of additional C-H···O4 hydrogen bonds. However, the resulting packing a small amount of leaves a small percentage of void (9.9% for **CP1** and 13.2% for **CP2**) occupied by disordered water molecules. Table S2 provides the more relevant coordination bond distances and angles, while Table S3 gathers the more relevant supramolecular interactions.

The crystal structure of **CP3** differs from the previous ones due to absence of the oxalate ligand and because of the distorted triangular coordination surrounding of the copper(I) center that reduces the dimensionality of the resulting coordination polymer from the previous 2D ones to the 1D nature of this latter compound (Fig. 4) [33]. The copper(I) metal centers are bridged by double monodentated μ-thymine-1-CH_2COO-κ*O*:κ*O* (3.0256(7) Å) ligands to generate Cu_2O_2 square planar cores which are linked by μ-4,4′-bpy-κ*N*:κN′ ligands to provide the linear 1D coordination polymer. The monodentate bridging mode of the thymine-1-acetato ligand is stabilized by the presence of an intramolecular C-H···O92 hydrogen bond. The geometry of the metal center belongs to a distorted triangular one with two oxygen atoms from the carboxylic group of two thymine-1-acetato ligands and a nitrogen atom from the 4,4′-bpy ligand. The mean plane of the thymine residues is almost perpendicular to the propagation direction. Again, the coordination polymers, chains in this case, are held together by means of complementary hydrogen bonding interactions (N3-H···O2) between the thymine residues of adjacent chains to create a supramolecular 2D layer. The final 3D crystal structure is achieved through π-π stacking interactions between the thymine residues and C-H···O4 hydrogen bonds involving the *bpy* ligand and the thymine residue.

3.2. Magnetic properties

Compound $[Cu_2(TAcO)_2(C_2O_4)(4,4'\text{-bpy})]\cdot 4H_2O$ (**CP1**) shows at room temperature a χ_mT value of ca. 0.6 $cm^3\,K\,mol^{-1}$, a value lower than the expected one for two non-interacting Cu(II) ions with g = 2 (the expected value is 0.75 $cm^3\,K\,mol^{-1}$). This lower value indicates that compound **CP1** presents a strong Cu—Cu antiferromagnetic interaction responsible for the observed decrease of the χ_mT value at room temperature. When the sample is cooled, χ_mT shows a continuous decrease to reach a plateau with a value close to 0.1 $cm^3\,K\,mol^{-1}$ below ca. 50 K (Fig. 5a). This behavior further confirms the presence of strong antiferromagnetic Cu—Cu interactions. The thermal variation of χ_m shows a rounded maximum at ca. 220 K, further suggesting the presence of a strong antiferromagnetic Cu—Cu interaction (Fig. 5b). Since the structure of **CP1** shows the presence of ladder chains where the rails are formed by Cu(II) ions connected through a *syn-anti* carboxylate bridge connecting an axial position with a basal one and the rungs are formed by oxalate bridges connecting basal positions, we can assume that the strong magnetic coupling must take place through the rungs of the ladder. Therefore, from the magnetic point of view we can consider compounds **CP1** as made up of oxalate-bridged Cu(II) dimers connected through a basal-axial *syn-anti* carboxylate bridge that is well known to give rise to weak magnetic couplings [34] Accordingly, we have fit the magnetic properties of **CP1** with the classical Bleaney-Bowers S = ½ dimer model [35]. This model (written as $H = -JS_1S_2$) reproduces very satisfactorily the magnetic properties of **CP1** with the following parameters: g = 2.215, J = −293 cm^{-1} and a 13.5% of a monomeric Cu(II) impurity accounting for the divergence of χ_m at low temperatures (Fig. 5b). The high and negative J value confirms the presence of a strong Cu—Cu interaction through the oxalate bridge. This high J value is very similar to those found in other square pyramidal Cu(II) complexes with a basal-basal oxalate bridge [36–39].

3.2.1. Electrical properties

The electrical conductivity of the CPs **1–3** in crystalline form was measured at 300 K, using the two-contact method. The data obtained 5.0×10^{-9}, 3.40×10^{-11}, 1.8×10^{-7} Scm^{-1} respectively, are in good agreement with a semiconductor behavior [21]. The conductivity values obtained are in accordance with previously reported CPs based on Cu(II) bearing pyridine bridge ligands with a long Cu(II) to Cu(II) distance, disadvantaging the mobility of electrons. The difference of two orders of magnitude in the electrical conductivity of **CP1** and **CP2** can be a consequence of the air instability of the **CP2** crystals. As

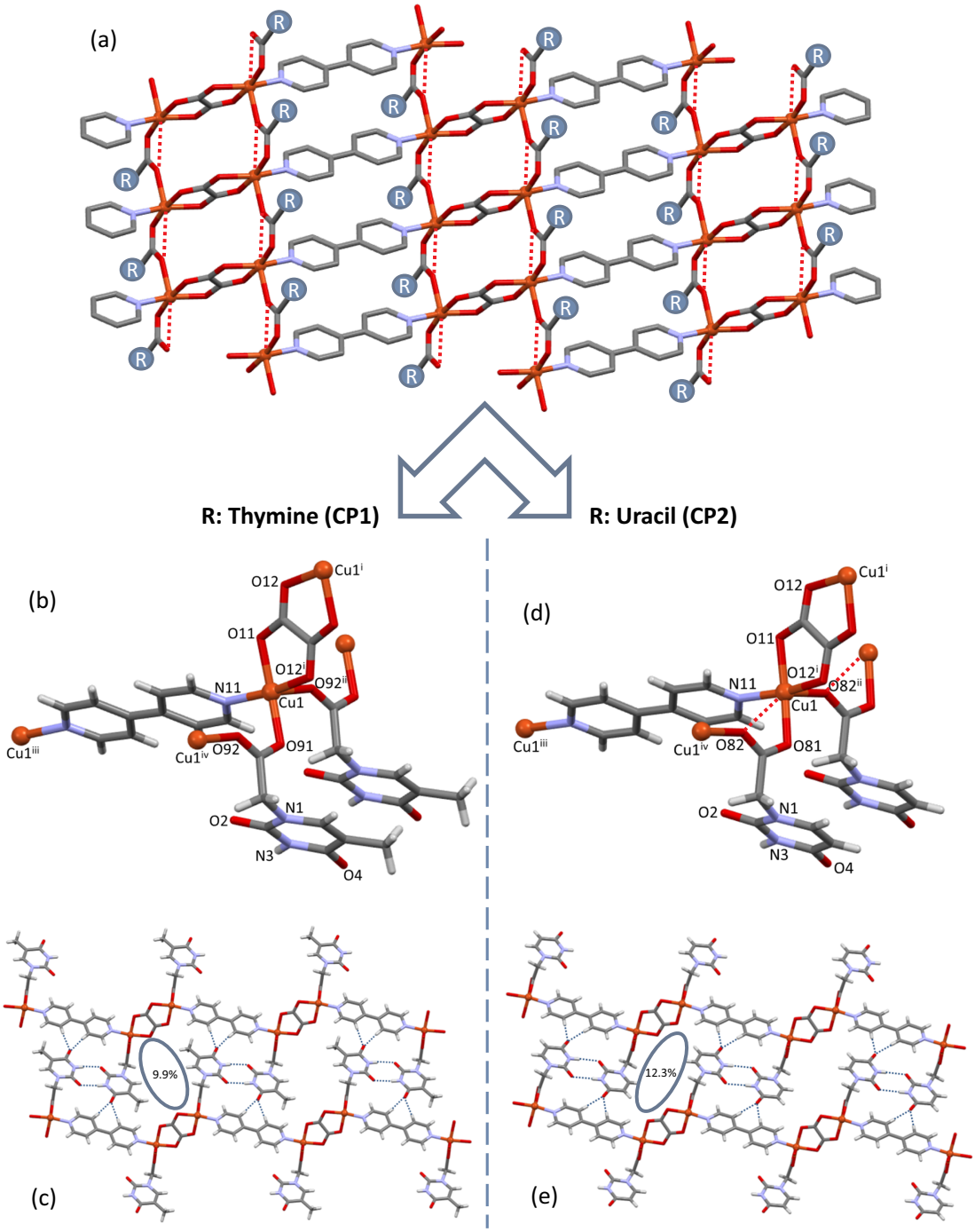

Fig. 3. (a) Shared molecular structure of the 2D coordination polymers **CP1** and **CP2**. Copper(II) coordination environment (b and d) and crystal packing (c and e). Blue dotted lines correspond to hydrogen bonds and red dashed ones to Cu···O semicoordination. (For interpretation of the references to colour in this figure legend, the reader is referred to the web version of this article.)

mentioned, the structure of **CP2** has larger voids (13.2%) that contain water molecules, than the corresponding **CP1** (9.9%). These data can justify the greater ease of **CP2** to lose these molecules, with the consequent loss of crystallinity, associated with a lower value in the electrical conductivity. To confirm the semiconductor behavior and to calculate de activation energy of **CP1**, its conductivity versus temperature has been studied (from 300 K to 380 K). At that temperature range the conductivity value increases two order of magnitude, from 5.1×10^{-9} at 300 K to 9.4×10^{-7} at 373 K [21], (Fig. S8) in agreement with it expected semiconductor behavior. In addition, the plot of conductivity (ln) versus 1/T (K), is almost linear and provides an activation energy of 0.84 eV over the given temperature range (Fig. S9).

The variation of electrical conductivity of the **CP1** on doping time with p-type oxidative dopant iodine was determined and the I-V curves of polymers are shown in (Fig. S10).

Iodine is usually employed as a mild oxidizing agent to seize electrons from the valence band of the semiconducting materials, in order to enhance their conductivity [21]. In the current case, the conductivity values of the doped sample increase by two orders of magnitude (Table 1). It can be assumed that the conductivity enhancement takes place through a mechanism involving an electronic charge transfer from the ligand to the oxidant. In general, on doping with iodine the

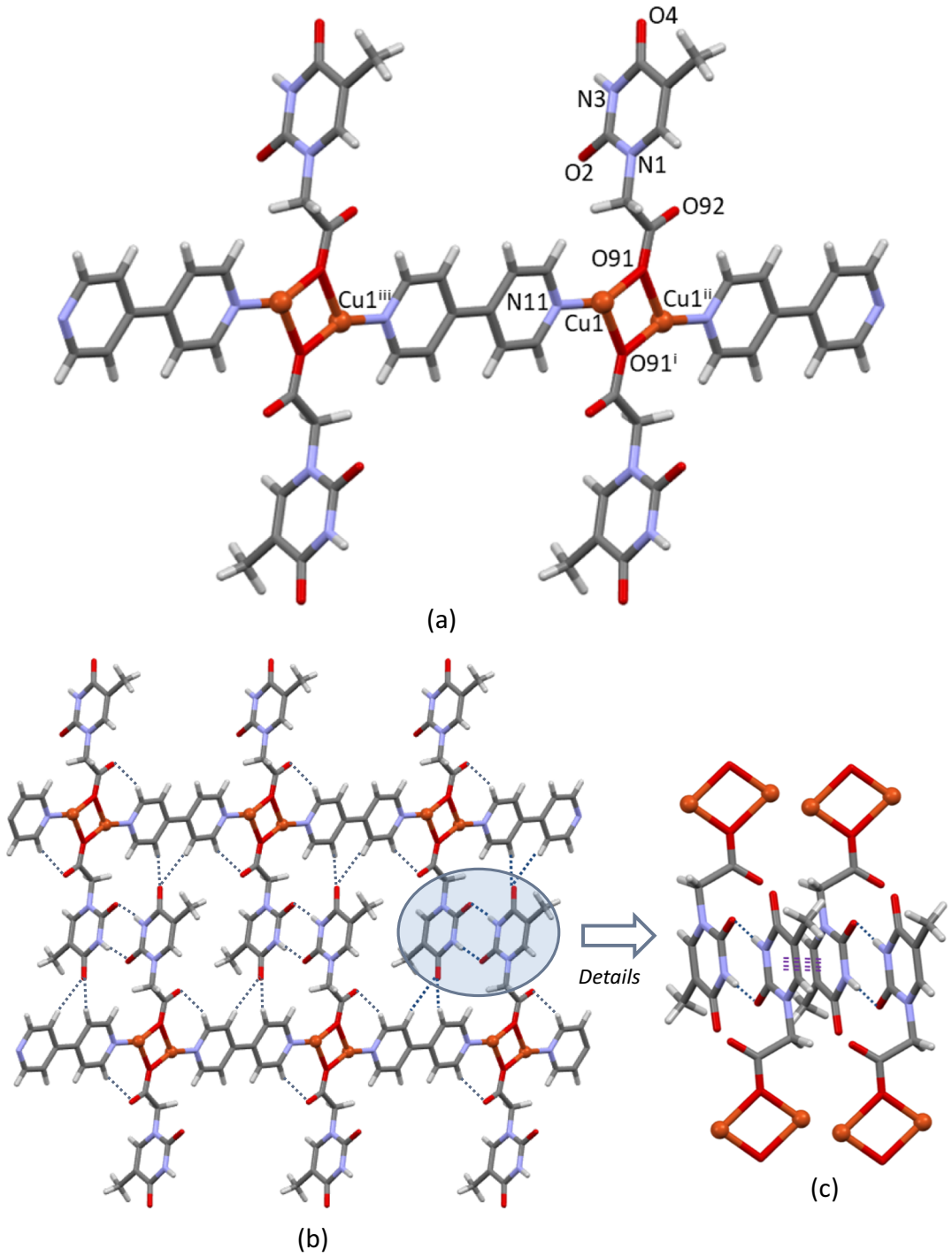

Fig. 4. (a) Fragment of the 1D coordination polymer **CP3**. Crystal packing (b) and supramolecular interactions (c). Copper(II) coordination environment (b and d) and crystal packing (c and e). Blue dotted lines correspond to hydrogen bonds and parallel purple lines indicate π-stacking interactions, (Tables S4 and S5 show selected bond lengths, angles and structural parameters for compound **CP3**). (For interpretation of the references to colour in this figure legend, the reader is referred to the web version of this article.)

electrons are removed from HOMO of ligand leaving positive holes with formation of I_3^- counter ions [40].

3.2.2. Nanoprocessing

As we have mentioned in the introduction, nanoprocessing CPs, (NCPs) is interesting from a biological or pharmacological point of view. The idea is developing highly tailorable functional materials that maintain the classical characteristic of bulk material with the advantages of nanometer features [41].

In this work, one of the presented coordination polymers (**CP1**) has been nanoprocessed, using a top-down approach [42] which consists in the miniaturization of bulk materials through cutting down. The decrease in size has been followed by scanning electron microscopy (SEM) (Fig. 6) and in all cases infrared spectroscopy (IR) and X-ray powder diffraction data (Figs. S11 and S12) of the sample has been performed in the successive steps, to confirm that the change obtained is only in

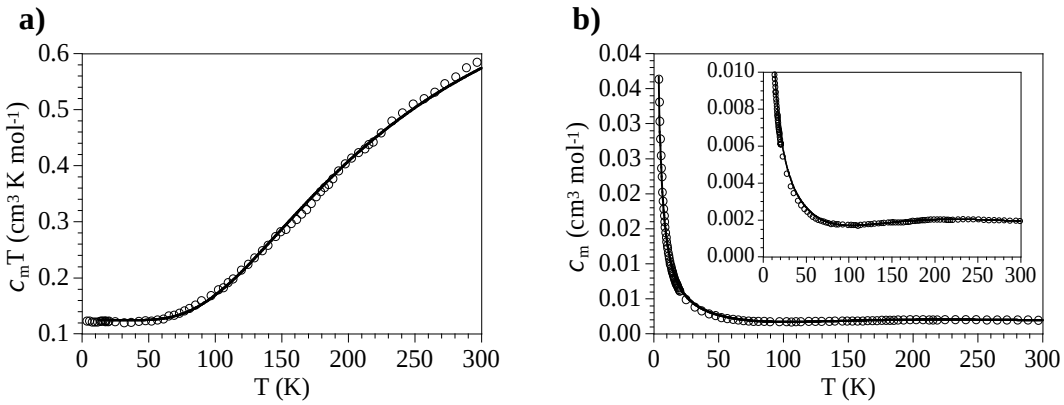

Fig. 5. Thermal variation of: (**a**) $\chi_m T$ and (**b**) χ_m per two copper(II) ions for **CP1**. Solid lines are the best fit to the models (see text).

Table 1
Electrical conductivity values obtained upon exposition of **CP1** doped with iodine (by solid-vapor treatment at different times, ambient temperature and pressure).

CP1 versus I_2 vapors (time min.)	Electrical conductivity (S/cm)
0	$5.0 \cdot 10^{-9}$
15	$2.1 \cdot 10^{-8}$
30	$3.3 \cdot 10^{-8}$
60	$8.0 \cdot 10^{-8}$
720	$9.9 \cdot 10^{-8}$
810	$1.0 \cdot 10^{-7}$

the dimension, and not in the structure (see materials and methods section). In this study, millimeter crystals long (2–2.6 mm) are used (Fig. 6a) and with the use of ultrasound (sonication in bath for 1 h at 37 kHz and 100 W of power), it is possible to decrease the size of the **CP1** until one micron long (Fig. 6b). In the supernatant suspension obtained after centrifuging for 2 min at 3000 rpm., still smaller flakes have been observed (approximately 200 nm width) (Fig. 6c). This proof of concept allows us to nanoprocess 55% of the initial material and shows that the use of ultrasound provides enough energy to break the weakest coordination bonds along the sheets and break the complementary hydrogen bonds establish between the thymine residues tethering the external surface of the **CP1**, which hold the 2D sheets.

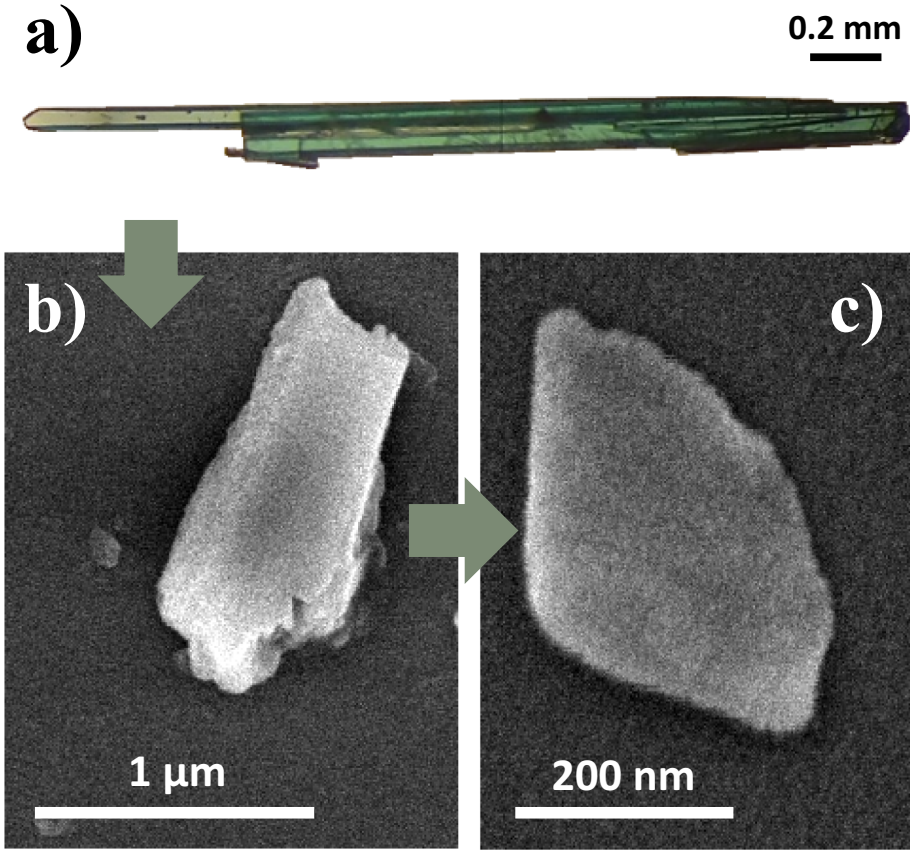

Fig. 6. a) This image corresponds to some original crystals of **CP1** with lengths between 2 and 2.6 mm approximately; **b**) after 1 h sonicated with ultrasonic bath; **c**) supernatant obtained after sonication 1 h and centrifuge at 3000 rpm for 2 min.

4. Conclusions

These studies, focused on CPs with nucleobases, easily nanoprocessable through top-down approaches, highlight the versatility of these compounds and their potential interest in biology, medicine or pharmacology.

It is corroborated that, apart from the adequate selection of the building blocks, the synthetic conditions are key for obtain new CPs with the possibility of modification of the ligands in situ, changes in the metal ion oxidation states and therefore in their structure and properties The presence of a metal cation is fundamental to obtain semiconductor coordination polymers that also respond to the presence of iodine vapors modifying their electrical conductivity, being also able to be used as sensors.

Acknowledgements

This work is dedicated to José Manuel Salas Peregrin.

This work has been funded by Universidad del País Vasco/Euskal Herriko Unibertsitatea (GIU17/50 and PP617/37), Gobierno Vasco (PIBA18-59) and Ministerio de Economía y Competitividad (MAT2016-75883-C2-1-P, CTQ2017-87201-P, MAT2016-75883-C2-2-P).

Appendix A. Supplementary data

Supplementary data to this article can be found online at https://doi.org/10.1016/j.jinorgbio.2019.110805.

References

[1] K.A. Siddiqui, J. Coord. Chem. 65 (2012) 4168–4176.
[2] A.N. Dou, Y.C. Du, Q.L. Chen, K.L. Luo, C. Zhang, A.X. Zhu, Q.X. Li, Z. Anorg. Allg. Chem. 642 (2016) 731–735.
[3] H. Thakkar, S. Eastman, Q. Al-Naddaf, A.A. Rownaghi, F. Rezaei, ACS Appl. Mater. Interfaces 9 (2017) 35905–35916.
[4] A. Angulo-Ibáñez, G. Beobide, O. Castillo, A. Luque, S. Pérez-Yánez, D. Vallejo-Sanchez, Polymers 8 (2016) 1–12.
[5] K.C. Stylianou, J.E. Warren, S.Y. Chong, J. Rabone, J. Bacsa, D. Bradshaw, M.J. Rosseinsky, Chem. Commun. 47 (2016) 3389–3391.
[6] V.G. Vegas, R. Lorca, A. Latorre, K. Hassanein, C.J. Gómez-García, O. Castillo, Á. Somoza, F. Zamora, P. Amo-Ochoa, Angew. Chem. Int. Ed. 56 (2017) 987–991.
[7] S. Pérez-Yáñez, G. Beobide, O. Castillo, J. Cepeda, A. Luque, P. Román, Cryst. Growth Des. 12 (2012) 3324–3334.
[8] P. Amo-Ochoa, F. Zamora, Coord. Chem. Rev. 276 (2014) 34–58.
[9] J. Troyano, O. Castillo, P. Amo-Ochoa, V. Fernández-Moreira, C.J. Gómez-García, F. Zamora, S. Delgado, J. Mater. Chem. C 4 (2016) 8545–8551.
[10] M. Hu, S. Ishihara, Y. Yamauchi, Angew. Chem. Int. Ed. 52 (2013) 1235–1239.
[11] V.G. Vegas, M. Villar-Alonso, C.J. Gómez-García, F. Zamora, P. Amo-Ochoa, Polymers 9 (2017) 1–13.
[12] E. Mateo-Martí, L. Welte, P. Amo-Ochoa, P.J.S. Miguel, J. Gómez-Herrero, J.A. Martin-Gago, F. Zamora, Chem. Commun. (2008) 945–947.
[13] D. Olea, S.S. Alexandre, P. Amo-Ochoa, A. Guijarro, F. de Jesús, J.M. Soler, P.J. de Pablo, F. Zamora, J. Gómez-Herrero, Adv. Mater. 17 (2005) 1761–1765.
[14] Y.-Y. Liu, Z.-X. Wang, X. He, M. Shao y M.-X. Li, Inorg. Chem. Commun. 80 (2005) 46–48.
[15] C.S. Hawes, P.E. Kruger, Aust. J. Chem. 66 (2013) 401–408.
[16] T. Okubo, N. Tanaka, K.H. Kim, H. Yone, M. Maekawa, T. Kuroda-Sowa, Inorg. Chem. 49 (2010) 3700–3702.
[17] M. Kurmoo, Chem. Soc. Rev. 38 (2009) 1353–1379.
[18] S. Delgado, P.J. Sanz Miguel, J.L. Priego, R. Jiménez-Aparicio, C.J. Gómez-García, F. Zamora, Inorg. Chem. 47 (2008) 9128–9130.
[19] P. Amo-Ochoa, S.S. Alexandre, S. Hribesh, M.A. Galindo, O. Castillo, C.J. Gómez-García, A.R. Pike, J.M. Soler, A. Houlton, R.W. Harrington, W. Clegg, F. Zamora, Inorg. Chem. 52 (2013) 5290–5299.
[20] J. Gómez-Herrero, F. Zamora, Adv. Mater. 23 (2011) 5311–5317.
[21] G. Givaja, P. Amo-Ochoa, C.J. Gómez-García, F. Zamora, Chem. Soc. Rev. 41 (2012) 115–147.
[22] X.-K. Yu, C.-J. Lin, Y.-Q. Zheng, H.-L. Zhu, Transit. Met. Chem. 39 (2014) 71–79.
[23] A. Sengupta, S. Datta, C. Su, T.S. Herng, J. Ding, J.J. Vittal, K.P. Loh, ACS Appl. Mater. Interfaces 8 (2016) 16154–16159.
[24] J. Xiong, M.-C. Liu, J.-X. Yuan, Acta Crystallogr. Sect. E: Struct. Rep. Online 61 (2005) o2665–o2667.
[25] A. Altomare, G. Cascarano, C. Giacovazzo, A. Guagliardi, M.C. Burla, G. Polidori, M. Camalli, J. Appl. Cristallogr. 26 (1993) 343–350.
[26] G.M. Sheldrick, Acta Crystallogr. Sect. C: Cryst. Struct. Commun. C71 (2015) 3–8.
[27] L.J. Farrugia, J. Appl. Crystallogr. 32 (1999) 837–838.
[28] G.A. Bain, J.F. Berry, J. Chem. Educ. 85 (2008) 532–536.
[29] G. Beobide, O. Castillo, J. Cepeda, A. Luque, S. Pérez-Yánez, P. Roman y J. Thomas-Gipson, Coord. Chem. Rev. 257 (2013) 2716–2736.
[30] H.-G. Jin, M.-F. Wang, X.-J. Hong, J. Yang, T. Li, Y.-J. Ou, L.-Z. Zhao, Y.-P. Cai, Inorg. Chem. Commun. 36 (2013) 236–240.
[31] M. Frisch, C.L. Cahill, J. Solid State Chem. 180 (2007) 2597–2602.
[32] X.-M. Chen, M.-L. Tong, Acc. Chem. Res. 40 (2007) 162–170.
[33] C.F. Macrae, I.J. Bruno, J.A. Chisholm, P.R. Edgington, P. McCabe, E. Pidcock, L. Rodriguez-Monge, R. Taylor, J. van de Streek, P.A. Wood, J. Appl. Crystallogr. 41 (2008) 466–470.
[34] B. Zhang, Y. Zhang, D. Zhu, Dalton Trans. 41 (2012) 8509–8511.
[35] B. Bleaney, K. Bowers, Proc. R. Soc. London, Ser. A 214 (1952) 451–465.
[36] D. Ghoshal, T.K. Maji, E. Zangrando, T. Mallah, É. Rivière, N.R. Chaudhuri, Inorg. Chim. Acta 357 (2004) 1031–1038.
[37] A. Escuer, M.S. El Fallah, R. Vicente, N. Sanz, M. Font-Bardía, X. Solans, F.A. Mautner, Dalton Trans. (2004) 1867–1872.
[38] R. Vicente, A. Escuer, J. Ferretjans, H. Stoeckli-Evans, X. Solans, M. Font-Bardía, J. Chem. Soc. Dalton Trans. (1997) 167–172.
[39] O. Kahn, Molecular Magnetism, VCH Publishers, USA, 1993.
[40] S. Anand, A. Muthusamy, J. Mol. Struct. 1148 (2017) 54–265.
[41] A. Carné, C. Carbonell, I. Imaz, D. Maspoch, Chem. Soc. Rev. 40 (2011) 291–305.
[42] Y. Lin, J.W. Connell, Nanoscale 4 (2012) 6908.